Monovalent, reduced-size quantum dots for imaging receptors on living cells

Mark Howarth[1,3], Wenhao Liu[1], Sujiet Puthenveetil[1], Yi Zheng[1], Lisa F Marshall[1], Michael M Schmidt[2], K Dane Wittrup[2], Moungi G Bawendi[1] & Alice Y Ting[1]

We describe a method to generate monovalent quantum dots (QDs) using agarose gel electrophoresis. We passivated QDs with a carboxy-terminated polyethylene-glycol ligand, yielding particles with half the diameter of commercial QDs, which we conjugated to a single copy of a high-affinity targeting moiety (monovalent streptavidin or antibody to carcinoembryonic antigen) to label cell-surface proteins. The small size improved access of QD-labeled glutamate receptors to neuronal synapses, and monovalency prevented EphA3 tyrosine kinase activation.

To perform single-molecule imaging in cells using dyes or fluorescent proteins, one must constantly contend with a weak signal, which typically bleaches in <10 s. Gold particles or latex beads allow stable single-particle tracking via their scattering, but are generally very large (30–500 nm)[1]. QDs are an alternative probe as they exhibit fluorescence so bright that single molecules can be imaged on an epifluorescence microscope, and their photostability allows hours of illumination without bleaching[2]. However, the full potential of QDs for cellular imaging has not yet been realized because of problems with large QD size (typically 20–30 nm for biocompatible red-emitting QDs[2]), the difficulty of delivering QDs into the cytosol, the instability of antibody-mediated targeting of QDs and QD multivalency. Previously we addressed the problem of binding instability by targeting streptavidin-functionalized QDs to cellular proteins that were site-specifically biotinylated by *E. coli* biotin ligase (BirA)[3]. In this work, we addressed QD multivalency and minimized the size of biomolecule-conjugated QDs (**Fig. 1a**).

QDs that are 20–30 nm can impair trafficking of proteins to which they are attached and restrict access to crowded cellular locations such as synapses[4]. A large fraction of QD size comes from the passivating layer, often a polyacrylic acid polymer or phospholipid micelle[2]. It is challenging to reduce the passivating layer without also increasing nonspecific interactions between QDs and cells, increasing QD self-aggregation and degrading quantum yield[5]. We previously synthesized a coating ligand for CdSe-ZnCdS core-shell QDs (**Supplementary Fig. 1** online) based on a dihydrolipoic acid (DHLA) head group to chelate the ZnCdS shell, 8 ethylene glycol (PEG) units to protect from nonspecific interactions, and a carboxylic acid tail to allow covalent coupling to biomolecules and to confer electrophoretic mobility[6,7]. When we used this DHLA-PEG_8-CO_2H ligand to coat 605 nm–emitting CdSe-ZnCdS QD cores (**Supplementary Methods** online), the resulting small QDs (sQDs) had a hydrodynamic diameter of 11.1 ± 0.1 nm, not much larger than an immunoglobulin gamma antibody (9.7 ± 0.1 nm; **Supplementary Fig. 2a** online). The quantum yield remained high (~40%), and the QDs were stable and monodispersed in PBS (**Supplementary Fig. 2**).

We tested whether the reduction in QD size improved access of the QDs to neuronal synapses. We fused the rat GluR2 subunit of the AMPA-type glutamate receptor, which localizes to postsynaptic membranes, to a 15-amino-acid 'acceptor peptide' (AP) recognition sequence for biotin ligase[3]. Instead of biotinylating the AP on the neuron surface with purified biotin ligase as in previous work[3], we used a simpler protocol in which we transfected neurons with plasmids encoding both AP-GluR2 and an endoplasmic reticulum (ER)-retained BirA construct (BirA-ER; **Supplementary Methods**). Using endogenous ATP and biotin, BirA-ER biotinylates AP-GluR2 in the secretory pathway (**Supplementary Fig. 3** online). We detected biotinylated AP-GluR2 with either streptavidin-conjugated sQDs or commercial streptavidin-QD605 (hydrodynamic diameter 21.2 ± 0.2 nm; **Supplementary Fig. 2a**) and compared the staining to the localization of a post-synaptic marker, Homer-GFP (**Fig. 1b**). AMPA receptors labeled with commercial QDs were hindered from entry into synapses (colocalization 24 ± 6%), whereas AMPA receptors labeled with the sQDs had significantly improved colocalization with the synaptic marker (colocalization 46 ± 7%, $P = 2.1 \times 10^{-4}$). As expected, AMPA receptors labeled using the small-molecule dye Alexa Fluor 568 gave the best colocalization (65 ± 17%).

QD multivalency is also a grave concern, as cross-linking of surface proteins can activate signaling pathways and dramatically reduce receptor mobility[1]. One approach to preparing monovalent nanoparticles had capitalized on the low density of functional sites on polystyrene beads, achieving ~70% monovalency[8,9]. Another approach had used nickel affinity separation, but there was overlap between monovalent and multivalent particles[10]. Nanoparticles have also been separated according to the number of DNA strands attached[11], but this adds a large size and promotes nonspecific binding to cells. Another potential solution is sub-stoichiometric derivatization so that most QDs have no ligand, some have one ligand and very few have two. However, this creates a large

[1]Department of Chemistry, [2]Department of Chemical Engineering and Division of Biological Engineering, 77 Massachusetts Avenue, Massachusetts Institute of Technology (MIT), Cambridge, Massachusetts 02139, USA. [3]Present address: Department of Biochemistry, South Parks Road, Oxford University, Oxford OX1 3QU, UK. Correspondence should be addressed to A.Y.T. (ating@mit.edu).

RECEIVED 7 NOVEMBER 2007; ACCEPTED 24 MARCH 2008; PUBLISHED ONLINE 20 APRIL 2008; DOI:10.1038/NMETH.1206

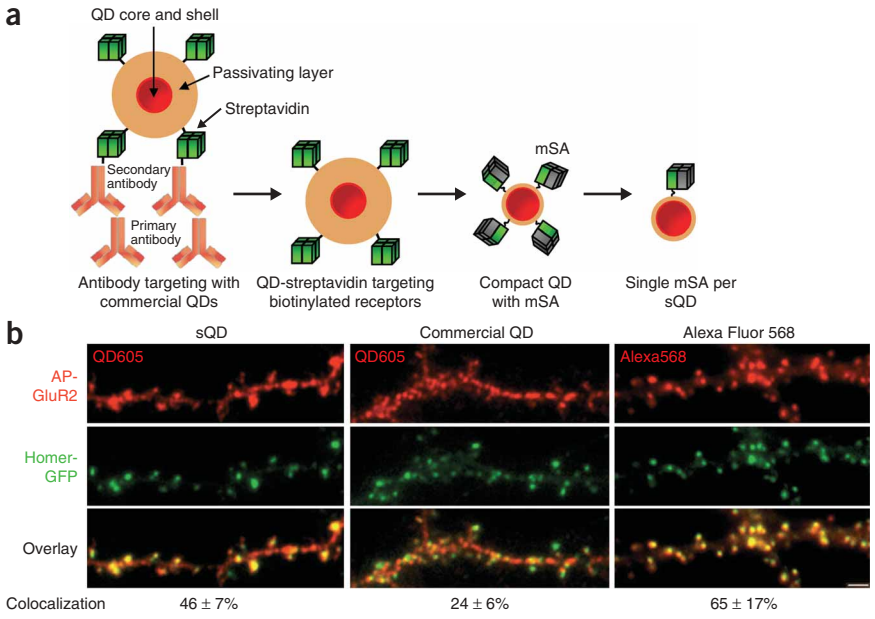

Figure 1 | Overview of small monovalent QDs, and accessibility of sQDs to synapses. (**a**) QDs are typically targeted to cell-surface proteins with antibodies (left), but streptavidin targeting reduces linkage size and increases stability. We decreased QD size by minimizing the passivating layer and reduced cross-linking by conjugating mSA. Finally we purified compact QDs (sQDs) bound to a single copy of mSA. (**b**) Fluorescence images of hippocampal neurons transfected with plasmids encoding AP-GluR2, BirA-ER and the post-synaptic marker Homer-GFP. Biotinylated AP-GluR2 was labeled at the cell surface with sQD-mSA$_1$, commercial QD605-streptavidin, or mSA–Alexa Fluor 568 and imaged live. Yellow shows the overlap between red QD- or Alexa-labeled GluR2, and green Homer puncta. Scale bar, 1 μm. Error, ± 1 s.d. ($n = 6$).

background of untargeted QDs that would be problematic for cytoplasmic labeling, for instance. A complete solution requires QDs uniformly functionalized with exactly one targeting group.

Commercial streptavidin-QD conjugates have 4–10 streptavidin molecules per QD, giving 16–40 biotin binding sites. To generate monovalent sQDs, we first replaced wild-type streptavidin with monovalent streptavidin (mSA), which we had previously engineered to contain a single femtomolar biotin binding site[12] (**Fig. 1a**). The next challenge was to conjugate a single mSA per sQD. Because of their negative charge (zeta-potential = –25 mV), sQDs move rapidly upon electrophoresis in an agarose gel, with comparable mobility to 1 kb DNA. When we conjugated sQDs to mSA and analyzed them by electrophoresis, we observed a striking ladder of QD mobility (**Fig. 2a**). Such a ladder has previously been observed after protein conjugation to QDs, but no purification or characterization had been shown[5,13]. We purified monovalent sQDs (sQD-mSA$_1$, where the subscript indicates the number of copies of mSA per sQD) from the gel by excising the band and centrifuging the sQDs out of the agarose (**Supplementary Methods**). Re-analysis of the purified sQD-mSA$_1$ by electrophoresis showed purity of > 95% (**Fig. 2a**). The hydrodynamic diameter of sQD-mSA$_1$ was 12.3 ± 0.2 nm (**Supplementary Fig. 2a**), only 1.2 nm greater than that of unconjugated sQDs. Although the multivalent metal-affinity interaction between the 6His tag of mSA and the sQD shell is not irreversible, sQD-mSA$_1$ was stable for >4 h at 37 °C as determined by gel electrophoresis and dynamic light scattering analysis (**Supplementary Fig. 4** online).

To test the valency of the gel-purified sQDs, we incubated them with mono-biotinylated DNA at various ratios and analyzed the conjugates by electrophoresis (**Supplementary Methods**). Unconjugated sQDs did not change in mobility, while sQD-mSA$_1$ shifted downward, giving a single new band at both low and high DNA concentrations, consistent with sQD monovalency (**Fig. 2b**). We also assessed valency by atomic force microscopy (AFM) of monovalent or multivalent sQDs (conjugated to ~6 copies of mSA) incubated with a threefold excess of mono-biotinylated DNA (**Fig. 2c** and **Supplementary Methods**). AFM showed monovalent sQD-mSA$_1$ particles bound to a single biotinylated DNA, but multivalent sQDs were bound to multiple DNA strands.

By imaging, we tested the impact of QD monovalency on EphA3, a receptor for ephrin involved in cell movement during development and metastasis. Previous work has shown that binding of EphA3 by multivalent ephrin-coated beads leads to EphA3 clustering and phosphorylation[14]. We labeled CHO cells expressing AP-tagged human EphA3 with either sQD-mSA$_1$ or multivalent sQDs (**Supplementary Methods**). sQD-mSA$_1$ labeled the receptor and remained diffusely localized, but multivalent sQDs clustered AP-EphA3 (**Fig. 3a**). In addition, significantly more EphA3 internalized upon labeling with multivalent sQDs (44 ± 11%)

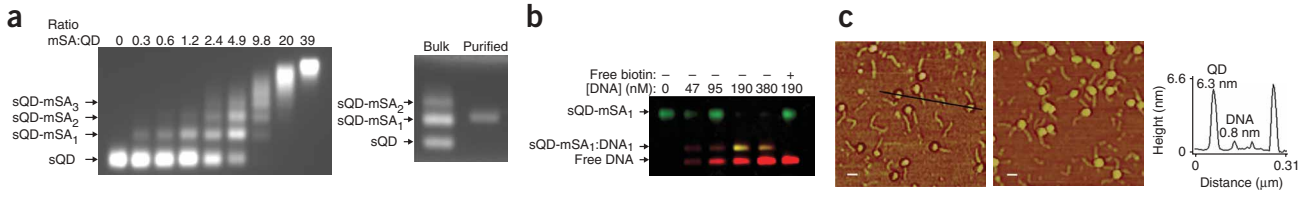

Figure 2 | Generation and characterization of monovalent sQDs. (**a**) sQDs were incubated with mSA, separated on an agarose gel according to the number of mSA molecules attached, and visualized under UV light (left). Discrete bands corresponding to 0–3 copies of mSA per sQD are indicated. sQD-mSA$_1$ was purified from a bulk mixture of sQD-mSA conjugates (right). (**b**) To test valency by gel shift, sQD-mSA$_1$ was incubated with mono-biotinylated DNA and analyzed by agarose gel electrophoresis. In the reaction shown in the rightmost lane, sQD-mSA$_1$ was pre-blocked with free biotin, to test the specificity of QD-DNA binding. QD emission is colored green, DNA is colored red, and yellow shows the overlap. (**c**) To test valency by AFM, purified sQD-mSA$_1$ (left) or multivalent sQDs (right) were incubated with threefold excess mono-biotinylated DNA and imaged by AFM. The height profile along the black line is plotted in the right panel. Scale bar, 25 nm.

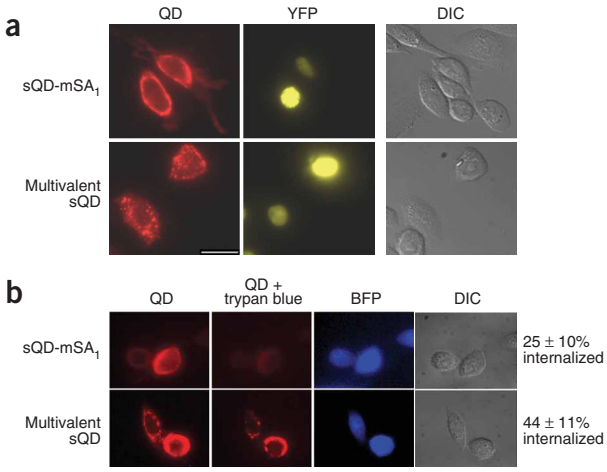

Figure 3 | Monovalent sQDs reduce EphA3 clustering and internalization. (**a**) CHO cells expressing AP-EphA3 were biotinylated and labeled with sQD-mSA$_1$ or multivalent sQDs for 14 min at 37 °C and were imaged live (left). YFP was used as a transfection marker and illustrates that sQD labeling is specific for transfected cells (middle). Differential interference contrast (DIC) images are shown on the right. (**b**) CHO cells expressing AP-EphA3 were biotinylated, incubated with sQD-mSA$_1$ or multivalent sQDs for 14 min at 37 °C, and imaged before and after quenching of surface sQDs with trypan blue. Blue fluorescent protein (BFP) was used as a transfection marker. The percentage internalized sQDs is given as the mean ± 1 s.d. ($n \geq 4$). Scale bars, 10 μm.

compared to sQD-mSA$_1$ (25 ± 10%, $P = 0.021$; **Fig. 3b**), as determined by the quenching of cell-surface sQDs with trypan blue, consistent with receptor activation by multivalent sQDs.

To demonstrate the generality of electrophoretic sQD purification, we also isolated sQDs bound to a single copy of a high-affinity antibody fragment against human carcinoembryonic antigen (CEA; **Supplementary Methods** and **Supplementary Fig. 5** online). We specifically labeled CHO cells expressing CEA with these monovalent anti-CEA sQDs. We found that proteins needed to be >50 kDa to allow electrophoretic separation of sQD conjugates according to valency (data not shown).

We applied sQD-mSA$_1$ to study the mobility of a mutant of low density lipoprotein (LDL) receptor with a truncated cytosolic tail, originally found from an individual with Familial Hypercholesterolemia. This mutant phenotype has been extensively investigated by following LDL, but we analyzed the behavior of the receptor itself (**Supplementary Methods**). We imaged single monovalent sQDs bound to the biotinylated AP-LDL receptor, as indicated by QD fluorescence intensity and blinking. The mobility of mutant receptors labeled with sQD-mSA$_1$ was significantly greater than that of labeled wild-type LDL receptor ($P = 1.6 \times 10^{-14}$; **Supplementary Fig. 6** and **Supplementary Videos 1** and **2** online), consistent with tethering of the wild-type cytosolic tail by adaptors in clathrin-coated pits[15].

Our method of monovalent QD separation has the advantages that it gives high purity, takes less than 30 min, uses commonly available equipment and should be applicable to any protein larger than 50 kDa. Electrophoretic separation also allows easy evaluation of the optimal ligand concentration and the success of the purification. One disadvantage of streptavidin-based protein tracking is that the expression level of the AP fusion protein must be well-controlled. However, our work here demonstrates a method to track endogenous cell-surface proteins without cross-linking, by purifying monovalent antibody-QD conjugates. Our strategy to make monovalent tight-binding QDs, using mSA, could be applied to other nanoparticles that show sufficient electrophoretic mobility. Controlled nanoparticle valency will also be advantageous *in vivo*, where cross-linking can trigger cell lysis, and for bottom-up nanotechnology. The combination of reduced size, monovalency and tight binding could help to make sQD-mSA$_1$ a standard tool for imaging protein dynamics at the single-molecule level.

Note: Supplementary information is available on the Nature Methods website.

ACKNOWLEDGMENTS

Funding was provided by the US National Institutes of Health (NIH) (P20GM072029-01), and the McKnight, the Dreyfus and the Sloan Foundations. M.H. was supported by an MIT-Merck fellowship, W.L. by a US National Science Foundation fellowship, M.G.B. by the Army Research Office DAAD 19-03-D0004, and K.D.W. and M.M.S. by the NIH (CA101830) and the MIT Biotechnology Training Program. We thank M. Lackmann, P. Janes, S. Manalis and A. Sparks for advice, J. Chan for technical assistance, and Tanabe for providing biotin.

AUTHOR CONTRIBUTIONS

M.H., W.L., M.G.B. and A.Y.T. designed the experiments; M.H. and A.Y.T. wrote the paper; M.H., W.L., S.P., L.F.M. and Y.Z. performed the experiments; M.M.S. and K.D.W. generated the PEG-scFv.

COMPETING INTERESTS STATEMENT

The authors declare competing financial interests: details accompany the full-text HTML version of the paper at http://www.nature.com/naturemethods/.

Published online at http://www.nature.com/naturemethods/
Reprints and permissions information is available online at http://npg.nature.com/reprintsandpermissions

1. Saxton, M.J. & Jacobson, K. *Annu. Rev. Biophys. Biomol. Struct.* **26**, 373–399 (1997).
2. Michalet, X. *et al. Science* **307**, 538–544 (2005).
3. Howarth, M., Takao, K., Hayashi, Y. & Ting, A.Y. *Proc. Natl. Acad. Sci. USA* **102**, 7583–7588 (2005).
4. Groc, L. *et al. J. Neurosci.* **27**, 12433–12437 (2007).
5. Pinaud, F., King, D., Moore, H.P. & Weiss, S. *J. Am. Chem. Soc.* **126**, 6115–6123 (2004).
6. Liu, W. *et al. J. Am. Chem. Soc.* **130**, 1274–1284 (2008).
7. Susumu, K. *et al. J. Am. Chem. Soc.* **129**, 13987–13996 (2007).
8. Worden, J.G., Shaffer, A.W. & Huo, Q. *Chem. Commun. (Camb.)* **7**, 518–519 (2004).
9. Sung, K.M., Mosley, D.W., Peelle, B.R., Zhang, S. & Jacobson, J.M. *J. Am. Chem. Soc.* **126**, 5064–5065 (2004).
10. Levy, R. *et al. ChemBioChem* **7**, 592–594 (2006).
11. Fu, A. *et al. J. Am. Chem. Soc.* **126**, 10832–10833 (2004).
12. Howarth, M. *et al. Nat. Methods* **3**, 267–273 (2006).
13. Pons, T., Uyeda, H.T., Medintz, I.L. & Mattoussi, H. *J. Phys. Chem. B.* **110**, 20308–20316 (2006).
14. Wimmer-Kleikamp, S.H., Janes, P.W., Squire, A., Bastiaens, P.I. & Lackmann, M. *J. Cell Biol.* **164**, 661–666 (2004).
15. Michaely, P., Li, W.P., Anderson, R.G., Cohen, J.C. & Hobbs, H.H. *J. Biol. Chem.* **279**, 34023–34031 (2004).